

# Catalytic enantioselective construction of tetrasubstituted carbons by self-assembled poly rare earth metal complexes

Masakatsu Shibasaki\* and Motomu Kanai

Received 27th March 2007

First published as an Advance Article on the web 10th May 2007

DOI: 10.1039/b704542e

Rare earth metal-based enantioselective catalysts that can promote practical cyanation reactions of ketones and ketoimines were developed. These catalytic enantioselective tetrasubstituted carbon-forming reactions are useful platforms for the synthesis of biologically active compounds. ESI-MS and crystallographic studies of the asymmetric catalysts revealed that the active catalysts are polymetallic complexes produced through the assembly of modules. The higher-order structure of the polymetallic complexes has strong effects on catalyst activity and enantioselectivity. Controlling the higher-order structure of artificial polymetallic asymmetric catalysts is a new strategy for optimizing asymmetric catalysts. Recent progress in this approach is also described.

## 1 Introduction

Asymmetric catalysis is a useful synthetic methodology.<sup>1</sup> In addition to high enantioselectivity, its robustness and user-friendliness are important requirements for asymmetric catalysts.

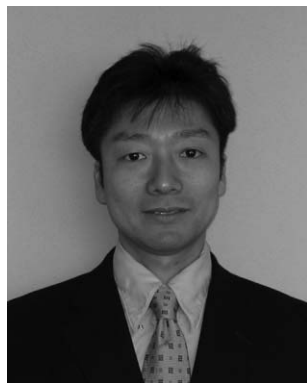
Asymmetric organocatalysis is an ideal approach in this direction.<sup>2</sup> Asymmetric, metal-based catalysts, however, are generally more reactive than organocatalysts, and promote various unique reaction patterns. Specifically, the high activity of metal-based asymmetric catalysts is usually required for tetrasubstituted carbon synthesis through carbon-carbon bond-formation to ketones and ketoimines.<sup>3,4,5</sup> Despite the existence of many catalytic asymmetric methods that produce chiral secondary alcohols and  $\alpha$ -secondary

Graduate School of Pharmaceutical Sciences, The University of Tokyo, 7-3-1 Hongo, Bunkyo-ku, Tokyo, 113-0033, Japan

*Masakatsu Shibasaki was born in 1947 in Saitama, Japan, and received his PhD from the University of Tokyo in 1974 under the direction of the late Professor Shun-ichi Yamada before doing postdoctoral studies with Professor E. J. Corey at Harvard University. In 1977 he returned to Japan and joined Teikyo University as an associate professor. In 1983 he moved to Sagami Chemical Research Center as a group leader, and in 1986 took up a professorship at Hokkaido University, before returning to the University of Tokyo as a professor in 1991. He was a visiting professor at Philipps-Universität Marburg during 1995. He has received the Pharmaceutical Society of Japan Award for Young Scientists (1981), Inoue Prize for Science (1994), Fluka Prize (Reagent of the Year, 1996), the Elsevier Award for Inventiveness in Organic Chemistry (1998), the Pharmaceutical Society of Japan Award (1999), the Molecular Chirality Award (1999), the Naito Foundation Research Prize for 2001 (2002), ACS Award (Arthur C. Cope Senior Scholar Award) (2002), the National Prize of Purple Ribbon (2003), the Toray Science Award (2004), The Japan Academy Prize (2005), Takamine Memorial Sankyo Award, 2006 (Japan), and the Rare Earth Society of Japan Award, 2006 (Japan). Moreover, he has been selected as a Fellow of the Royal Society of Chemistry (1997) and a Honorary Fellow of Chemical Research Society of India in 2003. His research interests include asymmetric catalysis and medicinal chemistry of biologically significant compounds.*



Masakatsu Shibasaki



Motomu Kanai

*Motomu Kanai was born in 1967 in Tokyo, Japan, and received his PhD from Osaka University in 1995 under the direction of Professor Kiyoshi Tomioka before doing postdoctoral studies with Professor Laura L. Kiessling at the University of Wisconsin. In 1997 he returned to Japan and joined Professor Shibasaki's group in the University of Tokyo as an assistant professor. He is currently an associate professor in Shibasaki's group. He has received the Pharmaceutical Society of Japan Award for Young Scientists (2001) and Merck-Banyu Lectureship Award (2005). His research interests entail design and synthesis of functional molecules.*

amines, catalytic construction of chiral tertiary alcohols and  $\alpha$ -tertiary amines is still an immature field. Considering the fact that there are a number of biologically active compounds, including drugs, that contain chiral tetrasubstituted carbons, developing practical asymmetric catalysts that can construct tetrasubstituted carbons is a demanding challenge.

To tackle this challenge, our basic concept for the catalyst design is a bifunctional asymmetric catalysis (Fig. 1).<sup>6</sup> Because many chemical reactions are bond-formations between nucleophiles and electrophiles, high enantioselectivity and catalyst activity can be expected if an asymmetric catalyst activates both of the reactants at the defined positions. There is a logical basis for using rare earth metals for bifunctional asymmetric catalysts. Rare earth metals contain the following characteristics, (1) moderate to high Lewis acidity, (2) high coordination numbers (up to 9), and (3) high ligand exchange rate. Due to the high coordination numbers [characteristic (2)], rare earth metal complexes tend to form aggregated polymeric structures, resulting in catalysts with multiple active sites. A Lewis acidic rare earth metal [characteristic (1)] can activate an electrophile, whereas another rare earth metal in the same polymeric complex can activate a nucleophile through, for example, transmetalation [characteristic (3)]. The rare earth metal complexes used in our studies are stable, and can tolerate a small amount of water and air.<sup>7</sup> In this perspective, we describe the development, application, structure, and mechanisms of the rare earth metal asymmetric catalysts that can promote tetrasubstituted carbon synthesis.<sup>8</sup>

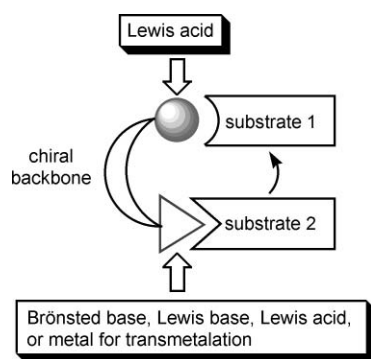


Fig. 1 Bifunctional asymmetric catalysis.

## 2 Catalytic enantioselective cyanosilylation of ketones

### 2.1 Reaction development

We developed the first general catalytic enantioselective cyanosilylation of ketones using a Ti complex generated from chiral ligands **1** and **2** (Table 1).<sup>9,10</sup> Those ligands were designed based on the concept of Lewis acid–Lewis base bifunctional asymmetric catalysis.<sup>6f</sup> Catalysts prepared from D-glucose-derived ligands **1** and **2** generally produced (*R*)-ketone cyanohydrins with high enantioselectivity [Table 1, eqn (1)]. Mechanistic studies, including control experiments using a catalyst without phosphine oxide, led us to propose the dual activation transition state model depicted as **6** in Fig. 2. TMSCN activated by the phosphine oxide would react with a ketone that was activated by Ti.

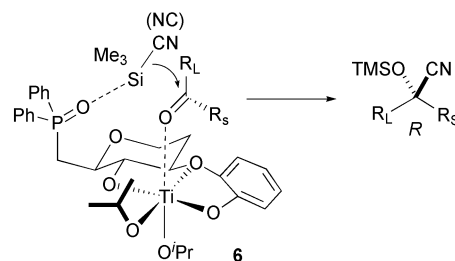
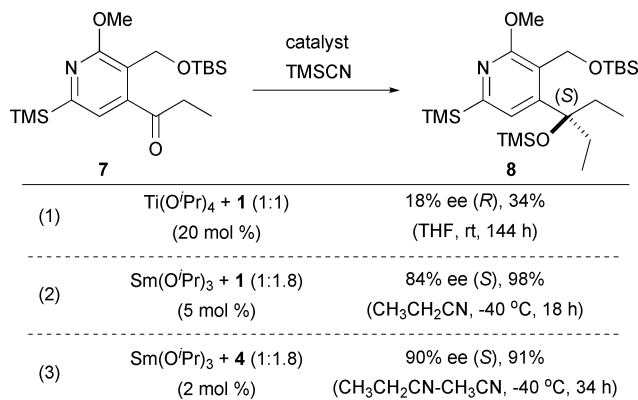


Fig. 2 Proposed transition state model for (*R*)-selective enantioselective cyanosilylation of ketones.

We planned to use this reaction as a platform for a catalytic asymmetric synthesis of camptothecin (**14**), anti-cancer drugs. The substrate (**7**, Scheme 1) for camptothecin synthesis has low reactivity because the ketone carbonyl is conjugated to an electron-rich pyridine containing a sterically bulky substituent at the *ortho*-position. As predicted, the reaction proceeded very sluggishly using 20 mol% of the Ti catalyst, and the corresponding (*R*)-ketone cyanohydrin (undesired configuration) was produced with low enantioselectivity [Scheme 1, eqn (1)].



Scheme 1 Platform reaction for the synthesis of camptothecin.

To overcome the low reactivity of **7**, we used a rare earth metal catalyst based on Utimoto's finding that rare earth metal alkoxides activate TMSCN through transmetalation, generating a highly nucleophilic rare earth metal cyanide species.<sup>11</sup> As expected, the reaction proceeded smoothly at -40 °C using a catalyst derived from Sm(O<sup>*i*</sup>Pr)<sub>3</sub> and **1** mixed in a 1 : 1.8 ratio. Unexpectedly, product **8** with the desired (*S*)-configuration was obtained with 84% ee [Scheme 1, eqn (2)]. The reaction conditions were optimized, and **8** was obtained with 90% ee using 2 mol% of catalyst derived from an electronically tuned ligand **4** [Scheme 1, eqn (3)].<sup>12</sup> Using this reaction as a key step, a versatile intermediate for camptothecin was synthesized.

Intrigued by the high catalyst activity and reversed enantioselectivity of the Sm catalyst, we next studied the substrate generality of the (*S*)-selective cyanosilylation of ketones.<sup>12a</sup> When using structurally simpler ketones, such as acetophenone, as the substrates, the corresponding Gd catalyst prepared from Gd(O<sup>*i*</sup>Pr)<sub>3</sub> and **1** in a 1 : 2 ratio produced higher enantioselectivity [Table 1, eqn (2)] than the Sm catalyst. Thus, it is possible to generally synthesize both enantiomers of ketone cyanohydrins using one chiral source derived from cheap D-glucose by changing the metal from Ti to a rare earth.

**Table 1** Catalytic enantioselective cyanosilylation of ketones

Entry	Ketone	Metal source	Ligand	Loading/x mol%	Temp/°C	Time/h	Yield (%)	Ee (%)
1		Ti(O <sup>i</sup> Pr) <sub>4</sub>	<b>2</b>	1	−20	88	92	94
2		Gd(O <sup>i</sup> Pr) <sub>3</sub>	<b>1</b>	1	−40	16	93	91
3		Ti(O <sup>i</sup> Pr) <sub>4</sub>	<b>2</b>	1	−25	92	72	90
4		Gd(O <sup>i</sup> Pr) <sub>3</sub>	<b>1</b>	5	−60	55	89	89
5		Ti(O <sup>i</sup> Pr) <sub>4</sub>	<b>2</b>	1	−10	92	90	92
6		Gd(O <sup>i</sup> Pr) <sub>3</sub>	<b>1</b>	5	−60	14	93	97
7		Ti(O <sup>i</sup> Pr) <sub>4</sub>	<b>1</b>	10	−50	88	72	91
8		Gd(O <sup>i</sup> Pr) <sub>3</sub>	<b>1</b>	5	−60	6.5	94	87
9		Ti(O <sup>i</sup> Pr) <sub>4</sub>	<b>2</b>	2.5	−30	92	72	90
10		Gd(O <sup>i</sup> Pr) <sub>3</sub>	<b>1</b>	5	−60	19	96	76
11		Ti(O <sup>i</sup> Pr) <sub>4</sub>	<b>2</b>	10	−50	36	92	85
12		Gd(O <sup>i</sup> Pr) <sub>3</sub>	<b>1</b>	5	−60	1	97	66
13		Ti(O <sup>i</sup> Pr) <sub>4</sub>	<b>2</b>	2.5	−45	92	80	82
14		Gd(O <sup>i</sup> Pr) <sub>3</sub>	<b>1</b>	5	−60	0.5	79	47

## 2.2 Reaction mechanism

Initial critical information about the composition of the asymmetric rare earth catalyst was obtained from the dependency of enantioselectivity on the mixed ratio of Gd(O<sup>i</sup>Pr)<sub>3</sub> and **1** in the catalyst preparation. The enantioselectivity increased according to the **1** : Gd ratio, producing maximum enantioselectivity at **1**/Gd = 2 (the optimized ratio). The enantioselectivity, however, almost saturated at **1**/Gd = 1.5. This dependency suggests that the active catalyst is a 2 : 3 complex of Gd and **1**.

The results of the following studies, addressing the relationship between enantioselectivity and the catalyst composition observed by ESI-MS, strongly support this hypothesis. When the Gd catalyst (prepared from Gd(O<sup>i</sup>Pr)<sub>3</sub> and **3** in a 1 : 2 ratio, catalyst A in Fig. 3) was applied to the cyanosilylation of **9**, a substrate for triazole antifungal (**15**) synthesis,<sup>13</sup> product **10** was obtained with only 68% ee. The enantioselectivity increased up to 83% when the catalyst was prepared from Gd{N(SiMe<sub>3</sub>)<sub>2</sub>}<sub>3</sub> and **3** in a 2 : 3 ratio (catalyst B). The difference was due to the purity of the catalytic species. A solution prepared from Gd(O<sup>i</sup>Pr)<sub>3</sub> and

**3** contained two main species: a 2 : 3 complex (**11** and **11** + **3**) and a 4 : 5 + oxo complex (Fig. 3a). By contrast, a *pre*-catalyst solution prepared from Gd{N(SiMe<sub>3</sub>)<sub>2</sub>}<sub>3</sub> contained a 2 : 3 complex (**11**) as the sole species (Fig. 3b). Because the enantioselectivity increased according to the concentration of the 2 : 3 complex, the 2 : 3 complex is likely to be the actual *pre*-catalyst. Importantly, the marked difference in enantioselectivity between the catalysts prepared from Gd(O<sup>i</sup>Pr)<sub>3</sub> and Gd{N(SiMe<sub>3</sub>)<sub>2</sub>}<sub>3</sub> was only observed when highly reactive ketones (such as **9**) were used as substrates. This finding suggests that the 4 : 5 + oxo complex would produce lower enantioselectivity, but with lower catalyst activity, than the 2 : 3 complex (see below).

The *pre*-catalyst (**11**) was subjected to the reaction conditions in the presence of excess TMSCN (Fig. 4). The Gd–O bond was cleaved by TMSCN, and gadolinium cyanide complex **12** with silylated ligands was observed by ESI-MS (data not shown, see ref 12a). <sup>1</sup>H NMR analysis of the recovered silylated ligand demonstrated that the phenolic oxygen atom was the silylation site. The generation of highly nucleophilic gadolinium cyanide in **12** suggests that the actual nucleophile was the gadolinium cyanide,

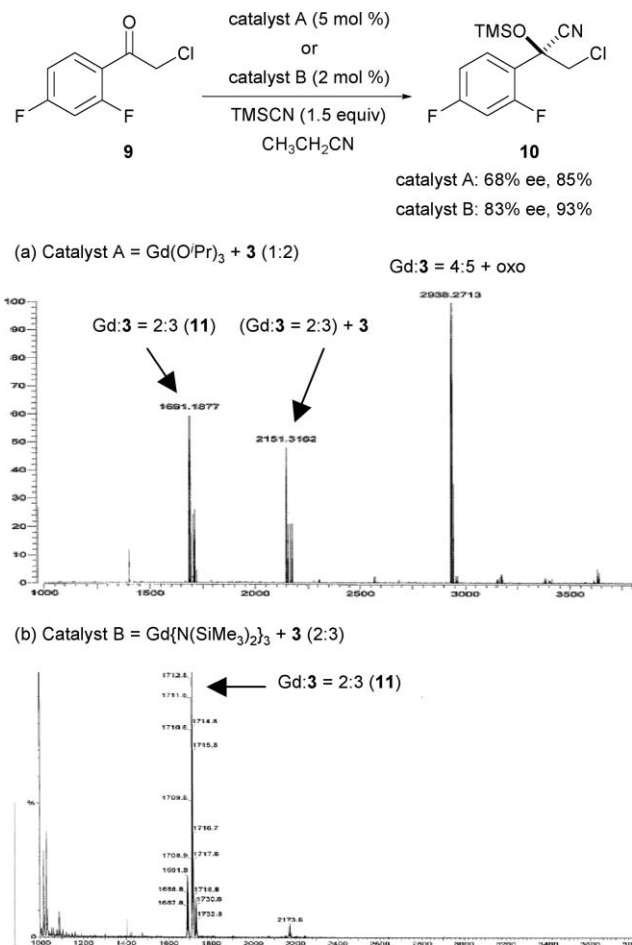


Fig. 3 Relationship between enantioselectivity and catalyst composition.

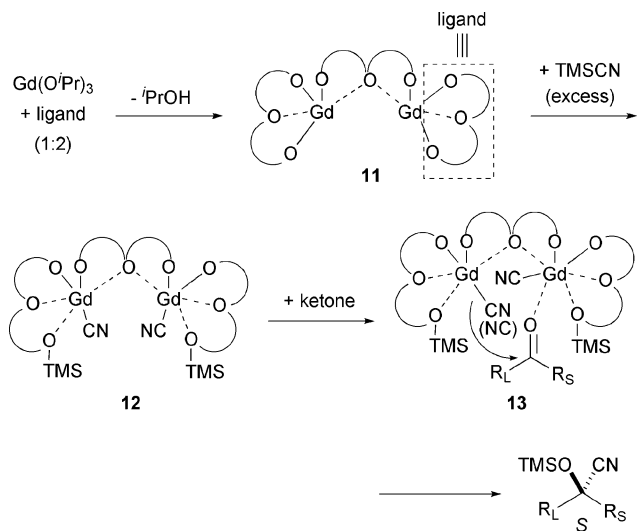


Fig. 4 Proposed catalyst structure and mechanism of (*S*)-selective Gd-catalyzed cyanosilylation of ketones.

not TMSCN. This hypothesis was supported by the following experiments. After generation of the  $^{13}\text{C}$ -labelled 2 : 3 complex using  $\text{TMS}^{13}\text{CN}$ , cyanosilylation was performed in the presence of variable amounts of  $\text{TMS}^{12}\text{CN}$ . The incorporation of  $^{13}\text{C}$  in the product was dependent on the ratio of  $^{13}\text{C}$  and  $^{12}\text{C}$  in the

reaction mixture. In addition, only one signal corresponding to CN was observed on the  $^{13}\text{C}$  NMR (117 ppm) analysis of **12** (the corresponding Pr complex, instead of the strongly paramagnetic Gd complex, was used in the NMR studies) labelled by  $^{13}\text{C}$  in the presence of variable amounts of  $\text{TMS}^{13}\text{CN}$  (0 or 2 equiv.) at  $-60^\circ\text{C}$ . These results confirmed the existence of a facile *pre*-equilibrium between gadolinium cyanide of the catalyst (**12**) and TMSCN. Kinetic studies were then conducted. The order dependency of the initial reaction rate on  $[\text{TMSCN}]$  and  $[\text{catalyst}]$  was determined to be 0 and 0.8, respectively. Therefore, the actual nucleophile is likely the gadolinium cyanide.

Combining the mechanistic information described above led us to propose a model **13** for the (*S*)-selective cyanosilylation of ketones promoted by the Gd catalyst (Fig. 4).<sup>12</sup> The reaction should proceed through an intramolecular cyanide transfer from a Gd to an activated ketone coordinating to the other Lewis acidic Gd of the bimetallic complex. The reversal of the enantioselectivity using either the Ti-catalyst or the Ln-catalyst resulted from differences in the catalyst structure and the reaction mechanism (Fig. 2 vs. Fig. 4).

The phosphine oxide of the ligand was essential for the high catalyst activity and enantioselectivity. The control catalyst, without phosphine oxide, produced significantly lower activity and enantioselectivity. No ESI-MS peaks were observed with the control catalyst, suggesting the lack of a defined structure. In addition, there was less gadolinium cyanide formation, based on the smaller amount of silylated ligand observed by  $^1\text{H}$  NMR. Therefore, the phosphine oxide probably stabilizes the active 2 : 3 complex, as well as facilitating the transmetalation for generation of the active nucleophile.

### 2.3 Synthetic applications

Catalytic enantioselective cyanosilylation of ketones is a powerful synthetic method. We have achieved asymmetric syntheses of versatile intermediates of camptothecins (**14**)<sup>12</sup> and triazole anti-fungals (**15**),<sup>13</sup> oxybutynin (**16**),<sup>14</sup> a neurokinin receptor antagonist (**17**),<sup>15</sup> and fostriecin (**18**) and 8-*epi*-fostriecin (**19**),<sup>16</sup> using catalytic cyanosilylation as a key step (Fig. 5). We describe here our latest achievement in this area—the catalytic asymmetric synthesis of fostriecin and 8-*epi*-fostriecin.

Fostriecin (**18**) is a secondary metabolite of *Streptomyces pul-veraceus* that exhibits potent anti-tumor activity through selective protein phosphatase 2A inhibition.<sup>17</sup> Due to its chemical structure and biological activity, fostriecin is an attractive synthetic target.<sup>18</sup> Our synthesis is unique due to the fact that four stereocenters were independently constructed using catalytic asymmetric reactions. This strategy is advantageous for the synthesis of stereo-analogues. Switching the enantioselectivity of each asymmetric catalyst allows for the synthesis of stereoisomers without changing the basic synthetic strategy. Specifically, we were interested in the effect of the chirality at the tetrasubstituted carbon C-8 on the biological activity. Generally, the chirality of tetrasubstituted carbons strongly influences on the global molecular structure.<sup>19</sup>

Thus, we achieved the synthesis of fostriecin using the (*R*)-selective Ti-catalyzed cyanosilylation of ketone **20** (5 mol% of Ti-2, 93% yield, 86% ee) as the initial key step. Synthesis of 8-*epi*-fostriecin (**19**) was also completed without significantly changing the synthetic route, starting from the (*S*)-selective Gd-catalyzed



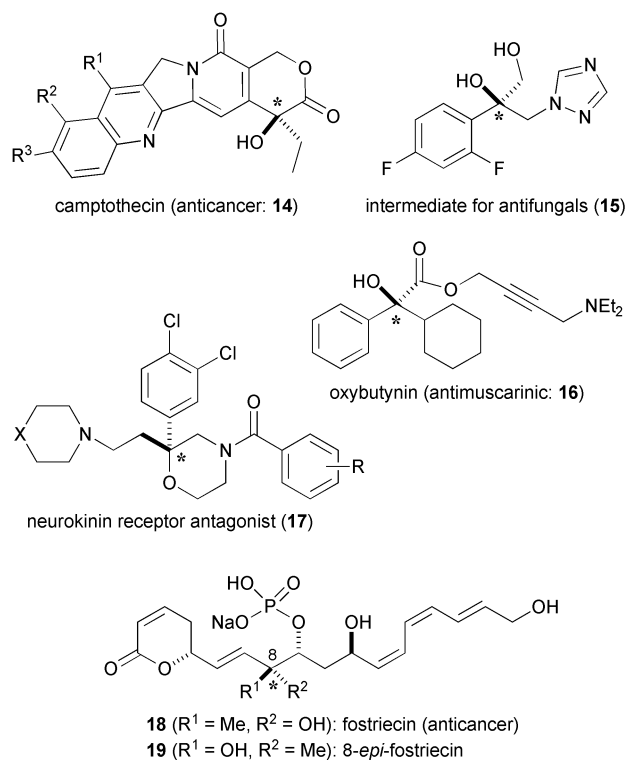


**Fig. 5** Synthetic targets of the catalytic enantioselective cyanosilylation of ketones.

cyanosilylation. Key steps for the 8-*epi*-fostriccin synthesis are shown in Scheme 2. The (*S*)-selective cyanosilylation of **20** proceeded in the presence of 2 mol% catalyst, producing cyanohydrin **21** in 95% yield with 86% ee. This reaction was performed in up to 120-g scale. **21** was converted to enantiomerically-pure aldehyde **22** *via* several operations, including recrystallization, which was subjected to a highly stereoselective (selectivity = 16 : 1) allylation using AgF-(*R*)-*p*-tol-BINAP catalyst developed by H. Yamamoto.<sup>20</sup> The chiral lactone was constructed from

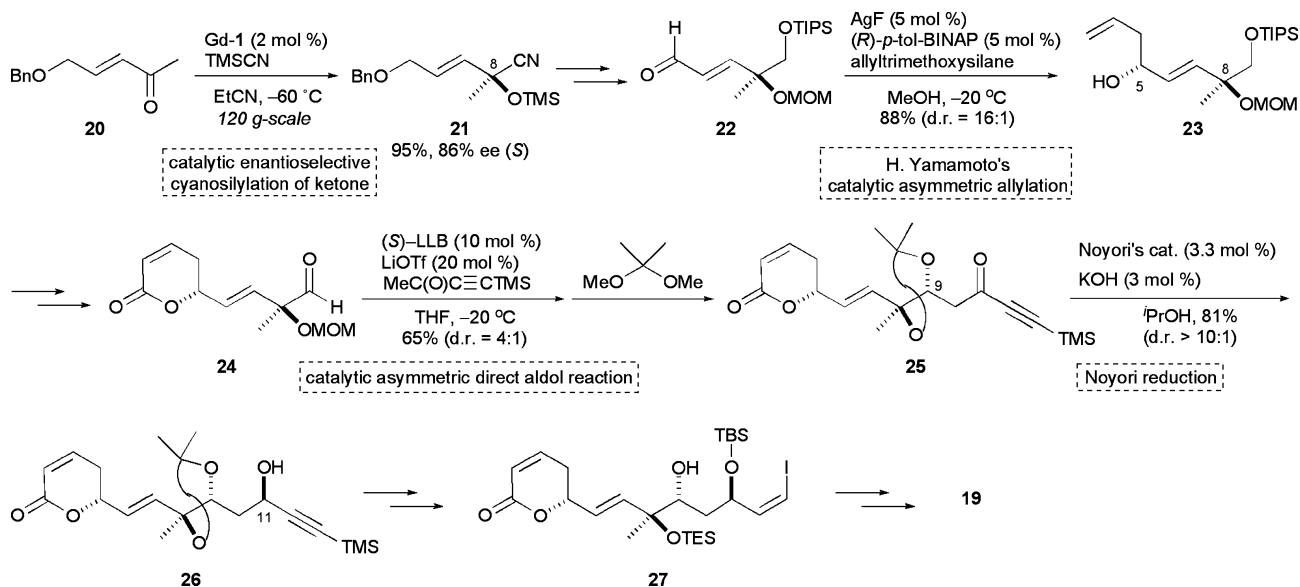
**23** through *O*-acryloylation followed by ring-closing metathesis. Aldehyde **24**, which was synthesized through subsequent deprotection and oxidation, was subjected to a catalytic asymmetric direct aldol reaction using (*S*)-LLB-LiOTf as an asymmetric catalyst<sup>21</sup> and an alkynyl ketone as a donor. Product **25** was obtained after protection in 65% yield with a diastereoselectivity of 4 : 1. It is noteworthy that this aldol reaction was very susceptible to a retro-aldol reaction under highly basic conditions. In fact, the aldol reaction *via* stoichiometric formation of the corresponding lithium enolate or zinc enolate of the alkynyl ketone did not afford the desired product. Only a bifunctional catalyst can provide such a base-sensitive aldol product.<sup>22</sup>

The final asymmetric induction was conducted under Noyori's transfer hydrogenation conditions, giving propargyl alcohol **26** with greater than 10 : 1 selectivity. At this stage, all of the stereogenic centers of 8-*epi*-fostriccin were constructed under catalyst control. Alkynylsilane **26** was converted to vinyl iodide **27** containing the appropriate protection pattern, which was subjected to the Stille cross-coupling reaction with a dienylstannane, and followed by phosphorylation and deprotection to produce 8-*epi*-fostriccin (**19**). Based on the protein phosphatase inhibition assay, 8-*epi*-fostriccin (**19**) was less active, but a more protein phosphatase 2A-selective inhibitor than fostriccin (**18**).<sup>16b</sup> This is the first biological study of fostriccin's stereo-analogues.

### 3 Catalytic enantioselective Strecker reaction of ketoimines

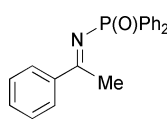
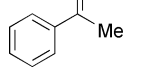
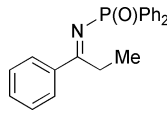
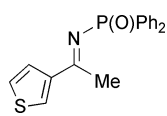
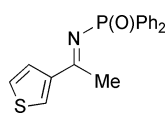
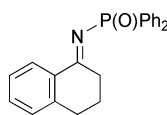
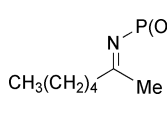
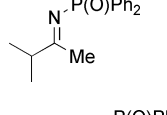
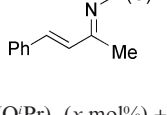
#### 3.1 Reaction development

Chiral  $\alpha,\alpha$ -disubstituted  $\alpha$ -amino acids are important building blocks for pharmaceuticals and artificially designed peptides.<sup>23</sup> The catalytic enantioselective Strecker reaction of ketoimines is one of the most direct and practical methods for the synthesis of this class of compounds.<sup>24</sup> Jacobsen's group developed an organocatalytic asymmetric Strecker reaction of aryl methyl and *tert*-butyl methyl ketoimines.<sup>3a,b</sup> Vallée *et al.* reported a



**Scheme 2** Catalytic asymmetric synthesis of 8-*epi*-fostriccin.

**Table 2** Catalytic enantioselective Strecker reaction of ketoimines

Entry	Substrate	Condition, <sup>a</sup> <i>x</i> = loading/mol%	Time/h	Yield (%)	Ee (%)
1		A (1)	30	94	92
2		B (0.1)	19	97	90
3		A (1)	31	97	95
4		A (1)	21	93	93
5		B (1)	3	99	99
6		A (1)	22	92	92
7		A (1)	43	73	90
8		A (2.5)	2.5	91	80
9		A (1)	38	93	96

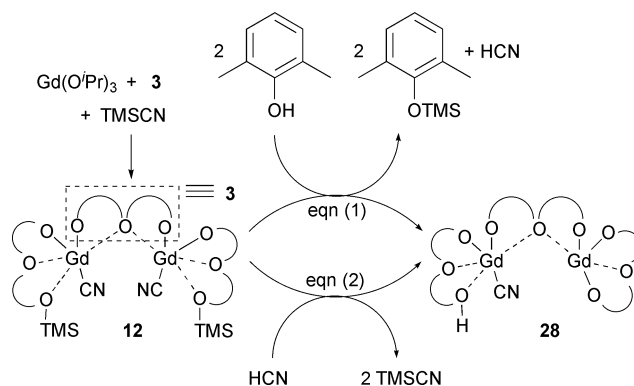
<sup>a</sup> Condition A: catalyst = Gd(O<sup>*i*</sup>Pr)<sub>3</sub> (*x* mol%) + **3** (2*x* mol%); TMSCN (1.5 equiv.), 2,6-dimethylphenol (1 equiv.). B: Catalyst = Gd(O<sup>*i*</sup>Pr)<sub>3</sub> (*x* mol%) + **3** (2*x* mol%); TMSCN (2.5–5 mol%), HCN (150 mol%).

reaction with an acetophenone-derived ketoimine, catalyzed by a chiral heterobimetallic complex.<sup>25</sup> We established the most general catalytic enantioselective Strecker reaction of phosphinoyl ketoimines using a Gd catalyst derived from ligand **3** in the presence of a protic additive (2,6-dimethylphenol or HCN).<sup>26</sup> Excellent enantioselectivity was produced from a wide range of substrates, including aromatic, heteroaromatic, cyclic, and aliphatic ketoimines (Table 2).

The protic additive significantly improved the catalyst activity as well as enantioselectivity. To gain insight into the additive effect, ESI-MS studies of the catalyst were performed in the presence of 2,6-dimethylphenol. A catalyst prepared from a 1 : 2 ratio of Gd(O<sup>*i*</sup>Pr)<sub>3</sub> and **3**, in the presence of TMSCN (15 equiv. to the catalyst) in acetonitrile, mainly afforded a peak corresponding to the *O*-silylated 2 : 3 complex (**12**). When 2,6-dimethylphenol (10 equiv.) was added to the catalyst solution, the peak corresponding to the 2 : 3 complex disappeared and a new peak corresponding to an *O*-protonated 2 : 3 complex (**28**) appeared [Scheme 3, eqn (1)]. Therefore, this protonated complex

was a highly active enantioselective catalyst in this asymmetric Strecker reaction of ketoimines.

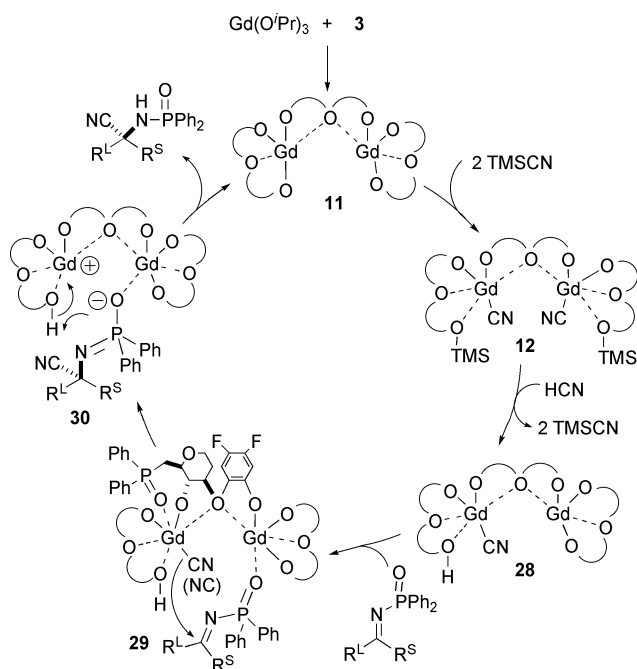
Based on this finding, we expected that the same active catalyst **28** would be generated through the reaction of HCN with **12**

**Scheme 3** Generation of protonated asymmetric catalyst.

[Scheme 3, eq. (2)]. Protonolysis with HCN produces 2 equiv. of TMSCN. Thus, only a catalytic amount of TMSCN is required if HCN is used as the proton source and stoichiometric cyanide source. This would lead to a more atom-economical catalytic enantioselective Strecker reaction.

As expected, the reaction proceeded smoothly in the presence of a catalytic amount of TMSCN and a stoichiometric amount of HCN (Table 2, condition B).<sup>26c</sup> The reaction time was significantly shortened compared to using 2,6-dimethylphenol as an additive (condition A). The higher reactivity allowed us to reduce the catalyst amount to as low as 0.1 mol%, while maintaining excellent enantioselectivity. The difference in reactivity when using HCN or 2,6-dimethylphenol as the proton source might be partly due to the acidity of the additive. In the presence of HCN ( $pK_a = 9.2$ ), the concentration of the active catalyst **28** should be higher than in the presence of 2,6-dimethylphenol ( $pK_a = 10$ ).

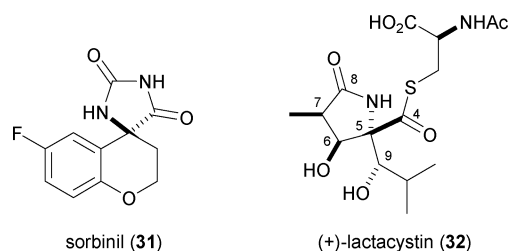
We propose the catalytic cycle shown in Scheme 4. To the active catalyst **28**, the substrate ketoimine is incorporated and activated. An intramolecular cyanide transfer from the gadolinium cyanide to the activated substrate defines the enantioselectivity (**29**), and the zwitterionic intermediate **30** is generated. In this step, the characteristics of phosphinoyl ketoimines—*i.e.*, the *cis/trans* isomers equilibrate very rapidly at the reaction temperature ( $-40\text{ }^\circ\text{C}$ )<sup>26a</sup>—should work advantageously in determining the reactive imine geometry. The intermediate **30** should collapse through intramolecular proton transfer, and the product was liberated with regeneration of gadolinium alkoxide complex **11**. From **11**, successive reactions with TMSCN and HCN reproduced the active catalyst **28**. The reaction did not proceed at all in the absence of a catalytic amount of TMSCN. This finding suggests that the active catalyst **28** is generated only through the silylated *pre-catalyst* **12**, and direct generation of **28** from the alkoxide complex **11** and HCN does not occur.



**Scheme 4** Proposed catalytic cycle of Strecker reaction of ketoimines.

## 3.2 Synthetic application

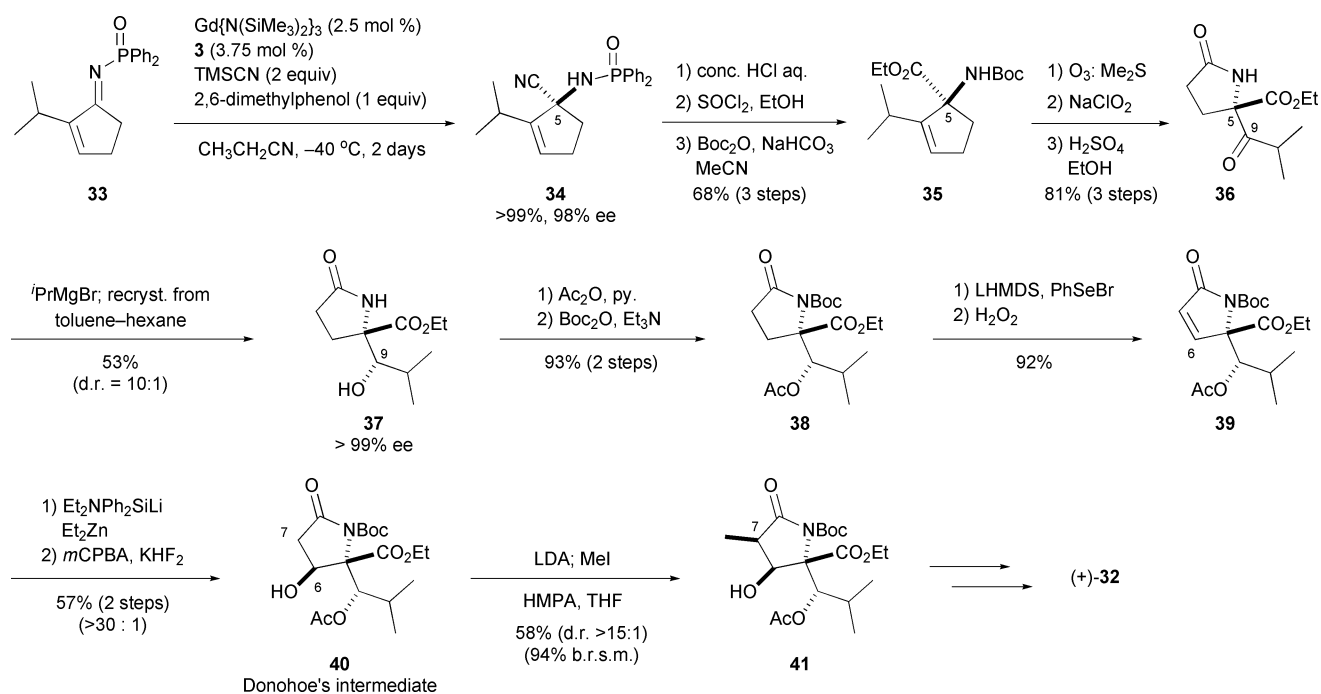
Due to the versatility of  $\alpha,\alpha$ -disubstituted amino acids in biologically active compounds, there are many potential synthetic targets for our reaction. We achieved catalytic asymmetric synthesis of sorbinil (**31**)<sup>26b</sup> and lactacystin (**32**)<sup>27</sup> using the catalytic enantioselective Strecker reaction of ketoimines. Here we describe our lactacystin synthesis.



(+)-Lactacystin (**32**) is a potent and selective proteasome inhibitor, isolated from the *Streptomyces* sp. by Omura *et al.*<sup>28</sup> Due to its potent biological activity and complex chemical structure, many synthetic chemists study **32** as a synthetic target.<sup>29</sup> We planned to utilize our catalytic enantioselective Strecker reaction for the construction of the tetrasubstituted carbon C-5 of lactacystin. Based on this plan,  $\alpha$ -hydroxy ketoimines are an obvious starting point. This type of imine, however, is unstable and not isolable in a pure form. Thus, we utilized an enone-derived, stable **33** as a masked  $\alpha$ -hydroxy ketoimine.

Imine **33**, containing a bulky isopropyl group at the  $\alpha$ -position, was barely reactive under the Strecker reaction conditions, and optimization of the reaction conditions was necessary. It was found that the catalyst generated from  $\text{Gd}\{\text{N}(\text{SiMe}_3)_2\}_3$  and **3** in a 2 : 3 ratio produced higher activity and enantioselectivity than the catalyst prepared from  $\text{Gd}(\text{O}^i\text{Pr})_3$ . The difference was attributed to the purity of the active 2 : 3 complex (Fig. 3). Under the optimized conditions, the Strecker reaction of **33** completed using 2.5 mol% catalyst in 2 days, and product **34** was obtained in quantitative yield with 98% ee (Scheme 5).

Amidonitrile **34** was converted to the protected amino acid derivative **35**, which was further transformed to  $\gamma$ -lactam **36** through ozonolysis, oxidation and cyclization. Stereoselective reduction of C-9 ketone using  $^i\text{PrMgBr}$ <sup>30</sup> via a presumed cyclic transition state produced a diastereomixture of C-9 secondary alcohols with the desired  $\alpha$ -alcohol **37** as the major isomer (*dr* = 10 : 1). Diastereomerically and enantiomerically pure **37** was obtained by recrystallization of the crude mixture from a toluene–hexane mixed solvent. After protection of the secondary alcohol and the lactam nitrogen atom with acetyl and Boc groups, respectively, selenenylation and oxidation of **38** produced the  $\alpha,\beta$ -unsaturated lactam **39** in excellent yield. The  $\beta$ -hydroxyl group of **39** was introduced via a stereoselective conjugate addition of the  $\text{Et}_2\text{NPh}_2\text{Si}$  group from the less hindered side of the enone, followed by Tamao–Fleming oxidation of the silicon with retention of configuration,<sup>31</sup> producing enantiomerically pure known intermediate **40**. Methylation at C-7 of **40** under the conditions developed by Donohoe<sup>32</sup> produced the desired stereoisomer **41**, which was further converted to lactacystin following the procedures reported by Corey and Donohoe.



**Scheme 5** Catalytic asymmetric total synthesis of lactacystin.

#### 4 Structural studies of the poly rare earth metal asymmetric catalysts

To elucidate the enantiodifferentiation mechanism of the asymmetric rare earth metal catalysts, we studied crystallization of the catalytic species by varying the ligand structure and metal. Colorless, air-stable prisms were obtained from a propionitrile-hexane (2 : 1) solution of the complex prepared from a 2 : 3 ratio of  $\text{Gd}(\text{O}^i\text{Pr})_3$  and ligand **5** (crystal **A**: 80% yield). X-Ray crystallographic analysis revealed that crystal **A** was a 4 : 5 complex of Gd and **5** with a  $\mu$ -oxo atom surrounded by four gadolinium atoms (Fig. 6).<sup>33</sup> The tetranuclear structure was maintained in a solution state, and the sole peak observed by ESI-MS corresponded to crystal **A**.

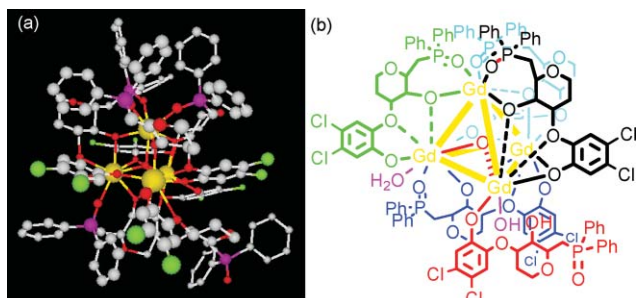


**Fig. 6** Crystal structure of 4 : 5 + oxo complex [crystal **A**] (a), and its chemical structure depiction (b).

Previously, the MS peak corresponding to crystal **A** was observed, concomitant with the 2 : 3 complex (active catalyst), in a solution prepared from a 1 : 2 ratio of  $\text{Gd}(\text{O}^i\text{Pr})_3$  and **5** (see Fig. 3a). The high yield of crystal **A** suggested that there is a

conversion process from the 2 : 3 complex to the 4 : 5 + oxo complex (crystal **A**) during crystallization. In addition, time-dependent conversion of the 2 : 3 complex to the 4 : 5 + oxo complex in a solution state was observed by ESI-MS. Moreover, this conversion was an autocatalytic process. Thus, seeding the 4 : 5 + oxo complex to a solution containing pure 2 : 3 complex (prepared from  $\text{Gd}\{\text{N}(\text{SiMe}_3)_2\}_3$ ) markedly accelerated the formation of the 4 : 5 + oxo complex. Therefore, the 4 : 5 + oxo complex is thermodynamically more stable than the active kinetically-formed catalyst, the 2 : 3 complex.

The function of crystal **A** as an enantioselective catalyst was evaluated by Strecker reaction of ketoimines. To our surprise, enantioselectivity was completely reversed when crystal **A** was used as a catalyst, compared to the catalyst prepared *in situ* (Table 3).<sup>33</sup> This dramatic reversal in enantioselectivity was attributed to the change in the higher-order structure of the chiral polymetallic catalyst. The reaction rate was approximately 5–50 times slower than that using the catalyst prepared *in situ*. Due to the marked difference in catalyst activity, the major enantiomer obtained using the catalyst prepared from  $\text{Gd}(\text{O}^i\text{Pr})_3$  was (*S*), whereas the catalyst solution contained a mixture of the 2 : 3 complex and the 4 : 5 + oxo complex.

Efforts to elucidate the structure of the active 2 : 3 complex continued. Colorless, air-stable prisms (crystal **B**) were obtained from a THF solution of  $\text{La}(\text{O}^i\text{Pr})_3$  and ligand **1** mixed in a 2 : 3 ratio (47% yield). The X-ray diffraction study revealed the structure to be a *pseudo*  $C_2$ -symmetric 6 : 8 complex of La and **1** (Fig. 7a).<sup>33</sup> Six La atoms were arranged in line as a backbone, and eight chiral ligands were arranged around the backbone. This structure was maintained in solution, based on the fact that the parent peak corresponding to crystal **B** was observed by ESI-QFT-MS (Fig. 7b). In addition, two major fragment peaks corresponding to metal : ligand = 2 : 3 and 4 : 5 + oxo complexes were observed.



**Table 3** Higher-order structure dependency of catalytic enantioselective Strecker reaction of ketoimines

Entry	Substrate	Catalyst <sup>a</sup>	Time/h	Yield (%)	Ee (%)	Configuration <sup>b</sup>
1		Gd-5	0.5	99	98	(S)
2		Crystal A	2	99	91	(R)
3		Gd-5	0.5	99	88	(S)
4		Crystal A	1	93	96	(R)
5		Gd-5	2	99	87	(S)
6		Crystal A	2	95	87	(R)
7		Gd-3	2.5	91	80	(S)
8		Crystal A	12	99	82	(R)
9		Gd-5	2	92	74	(S)
10		Crystal A	14	99	98	(R)

<sup>a</sup> Loading of Gd was 5 mol% in entries 1, 3 and 5, 2.5 mol% in entry 7, 10 mol% in entry 9, and 7 mol% in entries 2, 4, 6, 8 and 10. <sup>b</sup> Absolute configuration was determined in entries 3 and 4. In other entries, absolute configuration was temporarily assigned by analogy.

The ESI-MS fragment patterns of crystal **B** provide insight into the relevance of crystal **B** to the optimized Gd catalyst (2 : 3 complex) in solution. The observed MS-fragments (2 : 3 and 4 : 5 + oxo) can be viewed as subunits of the entire polymetallic assembly. The X-ray structure of crystal **B** supports this consideration: the distance between La<sup>2</sup> and La<sup>3</sup> atoms (or La<sup>4</sup> and La<sup>5</sup> atoms) was significantly longer than that between La<sup>1</sup> and La<sup>2</sup> (or La<sup>5</sup> and La<sup>6</sup>) (Fig. 7c). In addition, the coordination number of La<sup>3</sup> (and La<sup>4</sup>) was smaller than those of La<sup>1</sup> and La<sup>2</sup> (or La<sup>5</sup> and La<sup>6</sup>), which might induce Lewis base coordination to La<sup>3</sup> (or La<sup>4</sup>) and dissociation of the terminal 2 : 3 subunits. Thus, the 6 : 8 complex (crystal **B**) is likely to be constructed *via* assembly of the 2 : 3 subunit (the red part in Fig. 7c) and the 4 : 5 + oxo subunit (the blue part). The terminal 2 : 3 subunits of crystal **B** might correspond to the optimized active catalyst. This hypothesis is supported by the fact that crystal **B** (8 mol% La) promoted the catalytic enantioselective Strecker reaction of acetylthiophene-derived ketoimine, giving the product with 26% ee. Configuration of the major product was the same (S) as when using a catalyst prepared *in situ*. Crystal **B** produced a similar level of enantioselectivity as when using a catalyst prepared *in situ* from La(O<sup>i</sup>Pr)<sub>3</sub> and **1** (16% ee). Therefore, crystal **B** represents one of the structures of the lanthanum catalyst in solution.

Although the three-dimensional structure of the actual catalyst (2 : 3 complex) has yet to be clarified, these results demonstrated that the higher-order structure of an artificial asymmetric polymetallic catalyst is a determining factor of the function (enantioselectivity and activity) of the asymmetric catalysts.

## 5. Other utilities of the poly rare earth metal asymmetric catalysts

### 5.1. Catalytic enantioselective conjugate addition of cyanide to $\alpha,\beta$ -unsaturated *N*-acylpyrroles

The Gd catalyst promotes a general catalytic enantioselective conjugate addition of TMSCN to  $\alpha,\beta$ -unsaturated *N*-acylpyrroles.<sup>34</sup> This type of reaction is useful for the synthesis of chiral  $\gamma$ -amino acids. Prior to our contribution, Jacobsen's group reported the first catalytic enantioselective conjugate addition of cyanide using the chiral salen-Al complex.<sup>35</sup> Although excellent enantioselectivity was realized from  $\beta$ -aliphatic-substituted substrates, substrates with  $\beta$ -aryl or vinyl substituents were unreactive. Our catalyst has overcome this limitation, and products were obtained with high enantioselectivity from a wide range of substrates, including  $\beta$ -aliphatic, aromatic, and alkenyl *N*-acylpyrroles, in the presence of TMSCN and HCN (Scheme 6). Pharmaceuticals and their lead compounds, such as pregabalin (an anticonvulsant drug) and  $\beta$ -phenyl-GABA (an inhibitor in the nervous system), were synthesized using this reaction as the key step.

### 5.2. Catalytic asymmetric ring-opening reaction of *meso*-aziridines with TMSCN

We reported the first catalytic asymmetric ring-opening reaction of *meso*-aziridines by TMSCN using the Gd-3 complex (Scheme 7).<sup>36</sup> The addition of a catalytic amount of trifluoroacetic acid (TFA) reproducibly improved the enantioselectivity. Based on ESI-MS studies, TFA was incorporated in the catalyst complex. TFA is

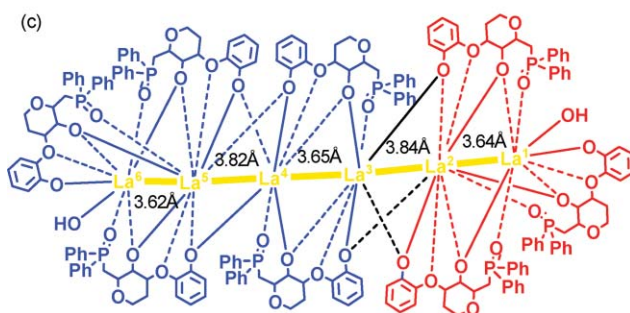
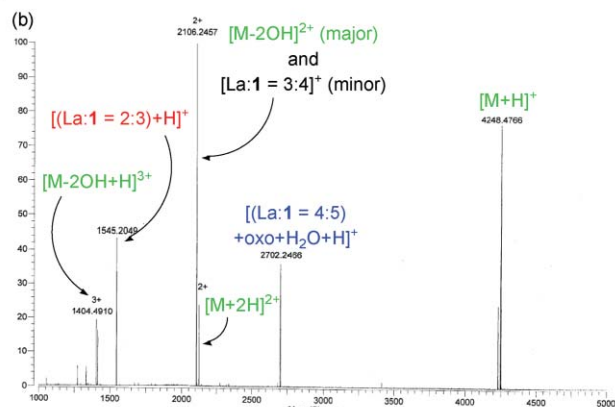
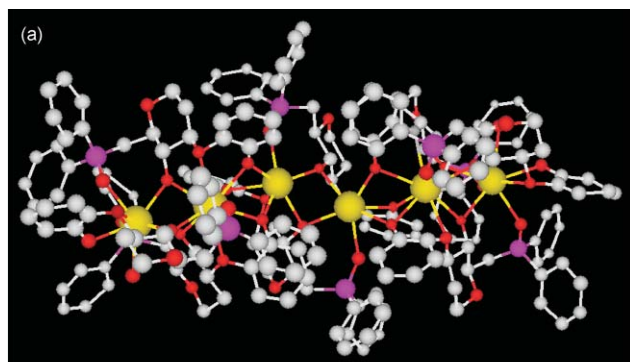
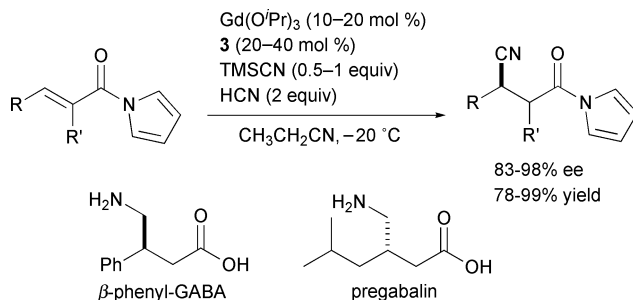
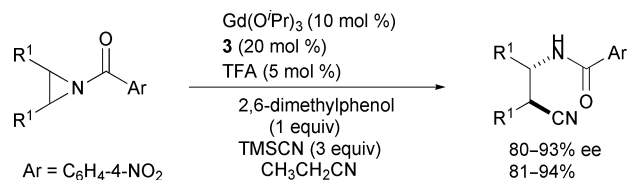


**Fig. 7** Crystal structure of 6 : 8 complex (crystal **B**) (a), ESI-QFT-MS of crystal **B** (b), and chemical structure depiction of crystal **B** (c).



**Scheme 6** Catalytic enantioselective conjugate addition of TMSCN to  $\alpha,\beta$ -unsaturated *N*-acylpyrroles.

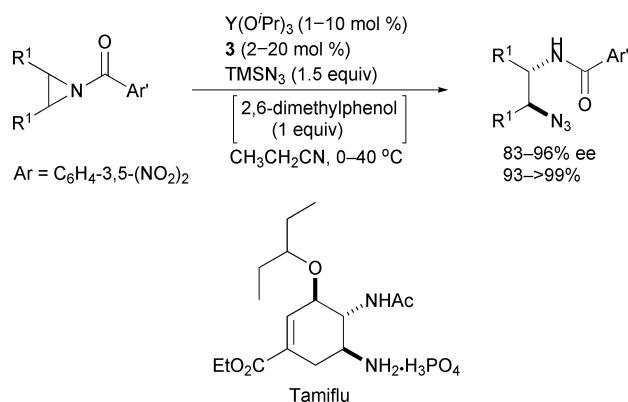
believed to bridge the two Gd atoms of the catalyst and stabilize the enantioselective polymeric complex. In addition, enhancement of the Lewis acidity of Gd, and fine-tuning of the relative positions of the two Gd atoms, might also contribute to the improved enantioselectivity. The ring-opened products were easily converted to chiral  $\beta$ -amino acids through acid hydrolysis.



**Scheme 7** Catalytic asymmetric ring-opening reaction of *meso*-aziridines with TMSCN.

### 5.3. Catalytic asymmetric ring-opening reaction of *meso*-aziridines with TMSN<sub>3</sub>

The yttrium catalyst prepared from Y(O<sup>*i*</sup>Pr)<sub>3</sub> and **3** in a 1 : 2 ratio promoted a general catalytic asymmetric ring-opening reaction of *meso*-aziridines with TMSN<sub>3</sub> (Scheme 8).<sup>37</sup> The products were direct precursors for enantiomerically enriched 1,2-diamines, versatile chiral building blocks for pharmaceuticals and chiral ligands. We utilized this reaction as a platform for our catalytic asymmetric synthesis of Tamiflu<sup>®</sup>, a very important anti-influenza drug.<sup>37,38</sup> In this synthesis, the aziridine opening reaction was performed in a 30 g-scale using 1 mol% of catalyst. The ligand was recovered through base extraction (without column chromatography) for reuse.



**Scheme 8** Catalytic asymmetric ring-opening reaction of *meso*-aziridines with TMSN<sub>3</sub>.

## 6. New design of poly rare earth metal asymmetric catalysts

The intimate relationship between higher-order structure and function of the asymmetric polymeric rare earth catalyst described in section 4 demonstrated the importance of controlling the catalyst's higher-order structure. Logical design of the higher-order structure, however, is difficult at this stage. Therefore, we plan to extract a structural module from the self-assembled polymeric complex (crystals **A** and **B**), and modify the module structure for the new catalyst design. We expected that the stabilization of the module will lead to a more stable higher-order structure. As a result, the active catalytic species should be unified, leading to higher catalyst activity and enantioselectivity.

Based on this assumption, we identified module **42** in the polymeric complexes derived from **1-5** (Fig. 8). In module **42**, a chiral ligand acts as a tetradentate ligand with each ligand bridging two rare earth metals (RE) by forming a 7-, 5-, and 5-membered fused chelation ring system. If the linker methylene between the

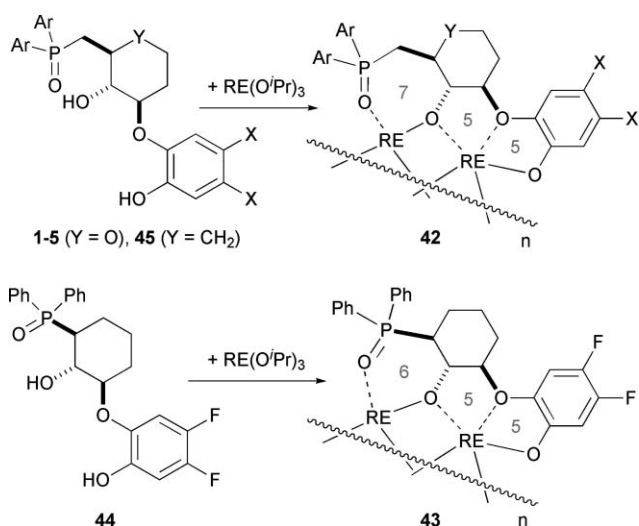


**Fig. 8** Schematic depiction of the module structure of polymetallic catalysts.

phosphine oxide and core tetrahydropyran ring is truncated, the resulting module contains a more stable 6-, 5- and 5-membered fused ring system (**43**). To avoid possible undesired phosphine oxide elimination *via* oxonium formation, we also changed the core structure from tetrahydropyran to cyclohexane. Thus, new module **43** and chiral ligand **44** were designed. Ligand **44** was readily synthesized *via* 5 steps from racemic 2-cyclohexen-1-ol using a dynamic kinetic resolution developed by Trost.<sup>39</sup>

The new catalyst prepared from **44** and Gd(O<sup>*i*</sup>Pr)<sub>3</sub> mixed in a 1 : 1.5 ratio was superior to the catalyst derived from **3** in the desymmetrization of *meso*-aziridines with TMSCN.<sup>40</sup> Both catalyst activity and enantioselectivity improved significantly (Table 4). The enantioselectivity was not dependent on the metal : ligand ratio used in catalyst preparation. Unexpectedly, the enantioselectivity was reversed compared to the catalyst derived from **3**, whereas **44** and **3** contained the same chirality. The enantio-switching was not due to the absence of the oxygen atom in the scaffolding 6-membered ring (tetrahydropyran *vs* cyclohexane); when using a catalyst prepared from Gd(O<sup>*i*</sup>Pr)<sub>3</sub> and control ligand **45** (10 mol%), the aziridine-opening product with the same absolute configuration as those obtained using sugar-derived ligand **3**, was produced. Therefore, the enantio-switching was attributed to the higher-order structural change induced by the one-carbon truncation between the phosphine oxide and the core 6-membered ring. The new catalyst was also effective in enantioselective conjugate addition of TMSCN to  $\alpha,\beta$ -unsaturated *N*-acylpyrroles.<sup>40b</sup>

To obtain further insight into the mechanism of the enantio-reversal, catalyst composition was studied by ESI-QFT-MS. A single peak corresponding to a **44**-Gd = 5 : 6 + oxo + OH complex was observed. Thus, the subtle change in the module structure (one-carbon difference in the linker) was amplified in the higher-order structure, and a completely different assembly state was produced.

Elucidation of the three-dimensional structure of the catalyst is currently ongoing. During this time, we succeeded in determining the crystal structure of the Gd-**44** = 3 : 4 + 2OH complex (Fig. 9). This crystal, however, was not the actual catalyst. Using the crystal

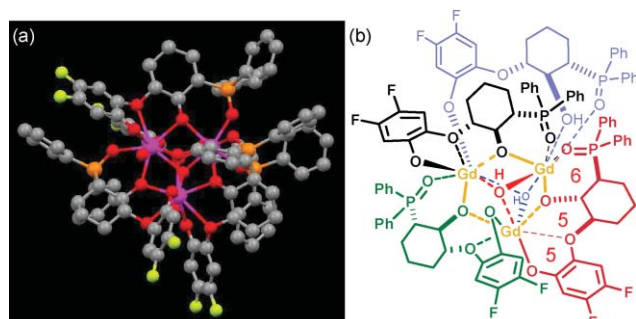


**Fig. 9** X-Ray structure of Gd-**44** = 3 : 4 + 2OH complex (a) and its chemical depiction (b).

as a catalyst, both enantioselectivity (62% ee from cyclohexene-derived aziridine, *cf.* Table 4, entry 1) and catalyst activity were significantly lower than those of the catalyst prepared *in situ*. We propose the term “assemblymer” to denote the relationship between the 5 : 6 + oxo + OH complex and the 3 : 4 + 2OH complex. These assemblymers contain the same module, but the modular assembly states (higher-order structure) are different. In this sense, the 2 : 3 complex and the 4 : 5 + oxo complex derived from the sugar-based ligands described in section 4 are also assemblymers. The assemblymers generally produce completely different catalytic functions.

The two assemblymers derived from **44** were interconvertible. The enantioselectivity recovered to 94% ee when Gd(O<sup>*i*</sup>Pr)<sub>3</sub> was added to the crystal (3 : 4 + 2OH complex) solution to adjust the Gd : ligand ratio to 5 : 6 and heated at 50 °C for 1 h before the reaction was conducted. Therefore, the highly enantioselective 5 : 6 + oxo + OH complex could be generated from the 3 : 4 + 2OH complex. In this case, the kinetically formed assemblymer (5 : 6 + oxo + OH complex) was more stable in a solution state than the assemblymer obtained through crystallization (3 : 4 + 2OH complex). Importantly, the crystal structure supports our initial hypothesis that the polymetallic complex is comprised of a stable 6-, 5-, and 5-membered fused chelation system. Further studies are ongoing to elucidate the actual catalyst structure and to extend the utility of the new catalyst.

## Conclusions

In this review, we described our development of asymmetric poly rare earth metal catalysts that can promote cyanation and azidation reactions, including cyanation of ketones and ketoimines (tetrasubstituted carbon-forming reactions). The reactions are practical, and used as key steps in catalytic asymmetric syntheses of several biologically active compounds.

Structural studies of the asymmetric catalyst revealed that the catalyst was a polymetallic rare earth complex constructed through the self-assembly of modules (Fig. 8, **42**). Two distinct higher-order structures were formed depending on the assembly state of the module, Gd : ligand = 2 : 3 complex and 4 : 5 + oxo complex. These two complexes can be selectively prepared either using Gd{N(SiMe<sub>3</sub>)<sub>2</sub>}<sub>3</sub> as the metal source for the 2 : 3 complex or crystallization for the 4 : 5 + oxo complex. These two “assemblymers” demonstrated completely distinct catalytic functions. Specifically, the enantioselectivity was reversed to an excellent level depending on the higher-order assembled structure

**Table 4** Catalytic asymmetric aziridine opening of *meso*-aziridines

Entry	Substrate	Ligand	Loading/ <i>x</i> mol%	Time/h	Yield (%)	Ee (%)
1		<b>44</b>	2	13	98	98
2 <sup>a</sup>		<b>3</b>	10	20	94	87
3		<b>44</b>	2	12	83	96
4 <sup>a</sup>		<b>3</b>	10	95	85	82
5		<b>44</b>	2	14	98	95
6 <sup>a</sup>		<b>3</b>	10	42	91	83
7		<b>44</b>	2	14	98	98
8 <sup>a</sup>		<b>3</b>	20	14	98	91
9		<b>44</b>	2	22	99	96
10 <sup>a</sup>		<b>3</b>	20	23	89	84
11		<b>44</b>	2	28	84	96
12 <sup>a</sup>		<b>3</b>	20	96	92	84
13		<b>44</b>	5	15	99	95
14 <sup>a</sup>		<b>3</b>	10	64	92	80
15		<b>44</b>	2	14	98	98
16 <sup>a</sup>		<b>3</b>	10	39	93	85

<sup>a</sup> Using a catalyst generated from *x* mol% of Gd(O<sup>*i*</sup>Pr)<sub>3</sub> and 2*x* mol% of **3** (*x* = 10 or 20) in the presence of 5 (or 2.5) mol% of TFA and 1 equiv. of 2,6-dimethylphenol. The absolute configuration of products was opposite to the one shown in the above scheme. See ref. 34.

of the catalyst in the Strecker reaction of ketoimines. The 2 : 3 complex afforded the (*S*)-products, while the 4 : 5 + oxo complex afforded the (*R*)-products. Therefore, the higher-order structure of the polymetallic catalyst is a determining factor of its function.

On the basis of this finding, we are currently investigating the logical design of higher-order structures of a polymetallic complex. Toward this goal, we started with tuning the module structure. This approach led us to identify a new polymetallic catalyst derived from ligand **44**. The higher-order structure of the catalyst derived from **44** appears to be more stable than those of catalysts derived from **1–5**. The new catalyst is markedly more effective in catalytic asymmetric aziridine-opening reactions with TMSCN. Efforts are ongoing to explore new asymmetric catalysts based on the logical design of the higher-order structure of the polymetallic catalysis.

## Acknowledgements

We acknowledge all the coauthors listed in the reference section for their supreme contribution to the achievements described in this review.

## References

- (a) *Comprehensive Asymmetric Catalysis*, ed. E. N. Jacobsen, A. Pfaltz and H. Yamamoto, Springer, Berlin, 1999; (b) I. Ojima, *Catalytic Asymmetric Synthesis*, 2nd edn, Wiley, New York, 2000.
- (a) *Asymmetric Organocatalysis*, ed. A. Berkessel and H. Gröger, Wiley-VCH, Weinheim, 2005; (b) *Acc. Chem. Res.* (Special Issue on Asymmetric Organocatalysis), ed. K. N. Houk and B. List, 2004, **37**, 487.
- Jacobsen's organocatalysts are exceptional in this sense. See: (a) P. Vachal and E. N. Jacobsen, *Org. Lett.*, 2000, **2**, 867; (b) P. Vachal and E. N. Jacobsen, *J. Am. Chem. Soc.*, 2002, **124**, 10012; (c) D. E. Fuerst and E. N. Jacobsen, *J. Am. Chem. Soc.*, 2005, **127**, 8964.
- To our knowledge, Fu's catalytic enantioselective alkylation of ketones is the first entry in this field. See: P. I. Dosa and G. C. Fu, *J. Am. Chem. Soc.*, 1998, **120**, 445.
- (a) E. J. Corey and A. Guzman-Perez, *Angew. Chem., Int. Ed.*, 1998, **37**, 388; (b) O. Riant and J. Hannedouche, *Org. Biomol. Chem.*, 2007, **5**, 873.
- (a) M. Shibasaki, H. Sasai and T. Arai, *Angew. Chem., Int. Ed. Engl.*, 1997, **36**, 1236; (b) G. J. Rowlands, *Tetrahedron*, 2001, **57**, 1865; (c) M. Shibasaki, M. Kanai and K. Funabashi, *Chem. Commun.*, 2002, 1989; (d) M. Shibasaki and N. Yoshikawa, *Chem. Rev.*, 2002, **102**, 2187; (e) J.-A. Ma and D. Cahard, *Angew. Chem., Int. Ed.*, 2004, **43**, 4566; (f) M. Kanai, N. Kato, E. Ichikawa and M. Shibasaki, *SYNLETT*, 2005, 1491; (g) T. Ikariya, M. Kuniyoshi and R. Noyori, *Org. Biomol. Chem.*, 2006, **4**, 393; (h) M. Shibasaki, M. Kanai and S. Matsunaga, *Aldrichimica*, 2006, **39**, 31.



- 7 For example, rare earth metals can be used as catalysts in water. See: (a) S. Kobayashi and I. Hachiya, *Tetrahedron Lett.*, 1992, **33**, 1625; (b) S. Kobayashi, S. Nagayama and T. Busujima, *J. Am. Chem. Soc.*, 1998, **120**, 8287; (c) S. Kobayashi and K. Manabe, *Acc. Chem. Res.*, 2002, **35**, 209; (d) S. Kobayashi and C. Ogawa, *Chem.–Eur. J.*, 2006, **12**, 5954; (e) S. Kobayashi, *Pure Appl. Chem.*, 2007, **79**, 235.
- 8 As a different approach for catalytic asymmetric construction of tetra-substituted carbons described in this review, we are also investigating Cu(I)-catalyzed reactions. See: (a) R. Wada, K. Oisaki, M. Kanai and M. Shibasaki, *J. Am. Chem. Soc.*, 2004, **126**, 8910; (b) R. Wada, T. Shibuguchi, S. Makino, K. Oisaki, M. Kanai and M. Shibasaki, *J. Am. Chem. Soc.*, 2006, **128**, 7687; (c) K. Oisaki, D. Zhao, M. Kanai and M. Shibasaki, *J. Am. Chem. Soc.*, 2006, **128**, 7164; (d) D. Zhao, K. Oisaki, M. Kanai and M. Shibasaki, *J. Am. Chem. Soc.*, 2006, **128**, 14440; (e) Y. Suto, M. Kanai and M. Shibasaki, *J. Am. Chem. Soc.*, 2007, **129**, 501. In addition, we reported a catalytic asymmetric retro-nitroaldol reaction that produces tetrasubstituted carbons through a kinetic resolution using a heterobimetallic rare earth complex: S.-y. Tosaki, K. Hara, V. Gnanadesikan, H. Morimoto, S. Harada, M. Sugita, N. Yamagiwa, S. Matsunaga and M. Shibasaki, *J. Am. Chem. Soc.*, 2006, **128**, 11776.
- 9 (a) Y. Hamashima, M. Kanai and M. Shibasaki, *J. Am. Chem. Soc.*, 2000, **121**, 7412; (b) Y. Hamashima, M. Kanai and M. Shibasaki, *Tetrahedron Lett.*, 2001, **42**, 691.
- 10 Catalytic enantioselective cyanosilylation of ketones reported by other groups: (a) Y. N. Belokon', B. Green, N. S. Ikonnikov, M. North and V. I. Tararov, *Tetrahedron Lett.*, 1999, **38**, 6669; (b) Y. N. Belokon', S. Caveda-Cepas, B. Green, N. S. Ikonnikov, V. N. Khrustalev, V. S. Larichev, M. A. Moscalenko, M. North, C. Orizu, V. I. Tararov, M. Tasinazzo, G. I. Timofeeva and L. V. Yashkina, *J. Am. Chem. Soc.*, 1999, **121**, 3968; (c) S.-K. Tian and L. Deng, *J. Am. Chem. Soc.*, 2001, **123**, 6195; (d) S.-K. Tian and L. Deng, *J. Am. Chem. Soc.*, 2003, **125**, 9900; (e) H. Deng, M. P. Isler, M. L. Snapper and A. H. Hoveyda, *Angew. Chem., Int. Ed.*, 2002, **41**, 1009; (f) D. H. Riu and E. J. Corey, *J. Am. Chem. Soc.*, 2005, **127**, 5384; (g) X. Liu, B. Qin, X. Zhou, B. He and X. Feng, *J. Am. Chem. Soc.*, 2005, **127**, 12224. See also ref. 3c.
- 11 S. Matsubara, H. Onishi and K. Utimoto, *Tetrahedron Lett.*, 1990, **31**, 6209.
- 12 (a) K. Yabu, S. Masumoto, S. Yamasaki, Y. Hamashima, M. Kanai, W. Du, D. P. Curran and M. Shibasaki, *J. Am. Chem. Soc.*, 2001, **123**, 9908; (b) K. Yabu, S. Masumoto, M. Kanai, D. P. Curran and M. Shibasaki, *Tetrahedron Lett.*, 2002, **43**, 2923; (c) K. Yabu, S. Masumoto, M. Kanai and M. Shibasaki, *Heterocycles*, 2003, **59**, 369.
- 13 M. Suzuki, N. Kato, M. Kanai and M. Shibasaki, *Org. Lett.*, 2005, **7**, 2527.
- 14 (a) S. Masumoto, M. Suzuki, M. Kanai and M. Shibasaki, *Tetrahedron Lett.*, 2002, **43**, 8647; (b) S. Masumoto, M. Suzuki, M. Kanai and M. Shibasaki, *Tetrahedron*, 2004, **60**, 10497.
- 15 M. Takamura, K. Yabu, T. Nishi, H. Yanagisawa, M. Kanai and M. Shibasaki, *SYNLETT*, 2003, 353.
- 16 (a) K. Fujii, K. Maki, M. Kanai and M. Shibasaki, *Org. Lett.*, 2003, **5**, 733; (b) K. Maki, R. Motoki, K. Fujii, M. Kanai, S. Kobayashi, S. Tamura and M. Shibasaki, *J. Am. Chem. Soc.*, 2005, **127**, 17111.
- 17 J. B. Tunac, B. D. Graham and W. E. Dobson, *J. Antibiot.*, 1983, **36**, 1595.
- 18 For a review of the total synthesis of fostriecin, see: M. Shibasaki and M. Kanai, *Heterocycles*, 2005, **66**, 727.
- 19 Fostriecin bends at the C-8 tetrasubstituted carbon. See: B. G. Lawhom, S. B. Boga, S. E. Wolkenberg, D. A. Colby, C.-M. Gauss, M. R. Swingle, L. Amable, R. E. Honkanen and D. L. Boger, *J. Am. Chem. Soc.*, 2006, **128**, 16720.
- 20 A. Yanagisawa, H. Kageyama, Y. Nakatsuka, K. Asakawa, Y. Matsumoto and H. Yamamoto, *Angew. Chem., Int. Ed.*, 1999, **38**, 3701.
- 21 (a) Y. M. A. Yamada, N. Yoshikawa, H. Sasai and M. Shibasaki, *Angew. Chem., Int. Ed. Engl.*, 1997, **36**, 1871; (b) LLB and LiOTf form oligomeric species. See: Y. Horiuchi, V. Gnanadesikan, T. Ohshima, H. Masu, K. Katagiri, Y. Sei, K. Yamaguchi and M. Shibasaki, *Chem.–Eur. J.*, 2005, **11**, 5195.
- 22 For other examples of catalytic asymmetric direct aldol reaction using an alkynyl ketone as a donor, see: (a) B. M. Trost, M. U. Frederikson, J. P. N. Papillon, P. E. Harrington, S. Shin and B. T. Shireman, *J. Am. Chem. Soc.*, 2005, **127**, 3666; (b) B. M. Trost, A. H. Weiss and A. J. von Wangelin, *J. Am. Chem. Soc.*, 2006, **128**, 8.
- 23 For reviews, see: (a) C. Cativiela and M. D. Diaz-de-Villegas, *Tetrahedron: Asymmetry*, 1998, **9**, 3517; (b) Y. Ohfuné and T. Shinada, *Bull. Chem. Soc. Jpn.*, 2003, **76**, 1115.
- 24 (a) H. Gröger, *Chem. Rev.*, 2003, **103**, 2795; (b) C. Spino, *Angew. Chem., Int. Ed.*, 2004, **43**, 1764.
- 25 M. Chavarot, J. J. Byrne, P. Y. Chavant and Y. Vallée, *Tetrahedron: Asymmetry*, 2001, **12**, 1147.
- 26 (a) S. Masumoto, H. Usuda, M. Suzuki, M. Kanai and M. Shibasaki, *J. Am. Chem. Soc.*, 2003, **125**, 5634; (b) N. Kato, M. Suzuki, M. Kanai and M. Shibasaki, *Tetrahedron Lett.*, 2004, **45**, 3147; (c) N. Kato, M. Suzuki, M. Kanai and M. Shibasaki, *Tetrahedron Lett.*, 2004, **45**, 3153.
- 27 N. Fukuda, K. Sasaki, T. V. R. S. Sastry, M. Kanai and M. Shibasaki, *J. Org. Chem.*, 2006, **71**, 1220.
- 28 S. Omura, T. Fujimoto, K. Otaguro, K. Matsuzaki, R. Moriguchi, H. Tanaka and Y. Sasaki, *J. Antibiot.*, 1991, **44**, 113.
- 29 For reviews of lactacystin synthesis, see: (a) M. Shibasaki, M. Kanai and N. Fukuda, *Chem.–Asian J.*, 2007, **2**, 20; (b) S. H. Kang, S. Y. Kang, H.-S. Lee and A. J. Buglass, *Chem. Rev.*, 2005, **105**, 4537; (c) C. E. Masse, A. J. Morgan, J. Adams and J. S. Panek, *Eur. J. Org. Chem.*, 2000, 2513; (d) E. J. Corey and W. Z. Li, *Chem. Pharm. Bull.*, 1999, **47**, 1.
- 30 S. H. Kang and H.-S. Jun, *Chem. Commun.*, 1998, 1929.
- 31 G. R. Jones and Y. Landais, *Tetrahedron*, 1996, **52**, 7599.
- 32 T. J. Donohoe, H. O. Sintim, L. Sisangia and D. J. Harling, *Angew. Chem., Int. Ed.*, 2004, **43**, 2293.
- 33 N. Kato, T. Mita, M. Kanai, B. Therrien, M. Kawano, K. Yamaguchi, H. Danjo, Y. Sei, A. Sato, A. Furusho and M. Shibasaki, *J. Am. Chem. Soc.*, 2006, **128**, 6768.
- 34 T. Mita, K. Sasaki, M. Kanai and M. Shibasaki, *J. Am. Chem. Soc.*, 2005, **127**, 514.
- 35 (a) G. M. Sammis and E. N. Jacobsen, *J. Am. Chem. Soc.*, 2003, **125**, 4442; (b) G. M. Sammis, H. Danjo and E. N. Jacobsen, *J. Am. Chem. Soc.*, 2004, **126**, 9928.
- 36 T. Mita, I. Fujimori, R. Wada, J. Wen, M. Kanai and M. Shibasaki, *J. Am. Chem. Soc.*, 2005, **127**, 11252.
- 37 Y. Fukuta, T. Mita, N. Fukuda, M. Kanai and M. Shibasaki, *J. Am. Chem. Soc.*, 2006, **128**, 6312.
- 38 (a) T. Mita, N. Fukuda, F. X. Roca, M. Kanai and M. Shibasaki, *Org. Lett.*, 2007, **9**, 259; (b) For other syntheses of Tamiflu®, see: S. Abrecht, P. Harrington, H. Iding, M. Karpf, R. Trussardi, B. Wirz and U. Zutter, *Chimia*, 2004, **58**, 621; (c) Y. Y. Yeung, S. Hong and E. J. Corey, *J. Am. Chem. Soc.*, 2006, **128**, 6310; (d) K. Yamatsugu, S. Kamijyo, Y. Suto, M. Kanai and M. Shibasaki, *Tetrahedron Lett.*, 2007, **48**, 1403.
- 39 B. M. Trost and M. G. Organ, *J. Am. Chem. Soc.*, 1994, **116**, 10320.
- 40 (a) I. Fujimori, T. Mita, K. Maki, M. Shiro, A. Sato, S. Furusho, M. Kanai and M. Shibasaki, *J. Am. Chem. Soc.*, 2006, **128**, 16438; (b) I. Fujimori, T. Mita, K. Maki, M. Shiro, A. Sato, S. Furusho, M. Kanai and M. Shibasaki, *Tetrahedron*, DOI: 10.1016/j.tet.2007.02.081.